Journal of Cleaner Production 201 (2018) 403–415

Contents lists available at ScienceDirect

Journal of Cleaner Production

journal homepage: www.elsevier.com/locate/jclepro

Responses of phosphorus use efficiency to human interference and climate change in the middle and lower reaches of the Yangtze River: Historical simulation and future projections

Jiazhong Zheng [a, b], Weiguang Wang [a, b, *], Xinchun Cao [a, c, d, **], Xiaozhou Feng [e], Wanqiu Xing [a, f], Yimin Ding [a, b], Qing Dong [a, b], Quanxi Shao [g]

[a] State Key Laboratory of Hydrology-Water Resources and Hydraulic Engineering, Hohai University, Nanjing 210098, China
[b] College of Hydrology and Water Resources, Hohai University, Nanjing 210098, China
[c] Key Laboratory of Efficient Irrigation-Drainage and Agricultural Soil-Water Environment in Southern China of Ministry of Education, Hohai University, Nanjing, Jiangsu 210098, China
[d] College of Agricultural Sciences and Engineering, Hohai University, Nanjing 210098, China
[e] Sanjiang University, Nanjing 210012, China
[f] School of Earth Sciences and Engineering, Hohai University, Nanjing 210098, China
[g] CSIRO Data 61, Private Bag 5, Wembley, Western Australia 6913, Australia

ARTICLE INFO

Article history:
Received 21 November 2017
Received in revised form
14 July 2018
Accepted 1 August 2018
Available online 4 August 2018

Keywords:
Substance flow analysis
Phosphorus use efficiency
Human interference
Climate change
Multiple neural networks
Global climate models

ABSTRACT

Phosphorus (P) is an indispensable resource for plant growth, and under the background with P consumption increase in crop system, the agriculture and crop production may be affected through the changes of phosphorus use efficiency (PUE) due to the human interference and climate change. Therefore, it is of great importance to investigate the responses of PUE to human interference and climate change from the perspectives of historical simulation and future projection. In this study, the changes of PUE from 2001 to 2015 in the middle and lower reaches of the Yangtze River (MLRYR) of China were evaluated by means of empirical PUE-model based on the substance flow analysis (SFA) method. Their responses to future human interference and climate scenarios during 2016–2030 were investigated by driving PUE-model with three neural networks (BP, GA-BP and PSO-BP) as well as the multiple downscaling climatic data (HadGEM2-ES, BCC-CSM1.1 (m) and GFDL-ESM2M) with the help of a statistical downscaling method (SDSM). The results showed that the PUE values of the three crops (rice, wheat and maize) were 53.61%, 36.22%, and 32.56%, respectively, during the period from 2001 to 2015 and 54.11%, 38.92% and 32.78%, respectively, during the period from 2016 to 2030. Consequently, the PUE showed an increasing trend from history to future. However, the overall PUE level was not high, with a value of not more than 60%, and notably for wheat and maize, the PUE was less than 40%. Meanwhile, the precipitation affected the leaching of P because increasing in precipitation may result in a relatively high increase in the probability of low-PUE. Moreover, great potential exists for enhancing the PUE in this region, and measures to improve PUE management practices have been proposed, such as, raising the crop yield, keeping the arable area and balancing the fertilization, etc. The present study provides a beneficial reference to comprehensively understand the impacts of human interference and climate change on the PUE and further improves regional sustainable strategies for future P resource management.

© 2018 Elsevier Ltd. All rights reserved.

1. Introduction

Playing a crucial role as a constituent of deoxyribonucleic acid (DNA) and adenosine triphosphate (ATP), phosphorus (P) is one of most essential elements for all forms of life on earth. Moreover, P has been applied as an important fertilizer to sustain crop growth

* Corresponding author. State Key Laboratory of Hydrology-Water Resources and Hydraulic Engineering Hohai University, Nanjing 210098, China.
** Corresponding author. State Key Laboratory of Hydrology-Water Resources and Hydraulic Engineering Hohai University, Nanjing 210098, China.
E-mail addresses: wangweiguang006@126.com (W. Wang), caoxinchun@hhu.edu.cn (X. Cao).

https://doi.org/10.1016/j.jclepro.2018.08.009
0959-6526/© 2018 Elsevier Ltd. All rights reserved.

since the last century (Cordell et al., 2009; Schmid Neset et al., 2008). However, as a nonrenewable resource, P does not have a rapid global cycle akin to the circulations of C and N. P fertilizer exists in the earth's crust in the form of phosphate rock, and it is only through weathering and leaching that P is mobilized into terrestrial systems (Suh and Yee, 2011). According to the assessment of worldwide reserves of rock phosphate from the International Fertilizer Development Center (IFDC), global phosphate rock reserves are estimated to run out over the next 70–140 years (Scholz et al., 2013; Vaccari, 2011). Nevertheless, with the world population growth and food consumption rising, demands for P fertilizer are expected to continue to increase (Smit et al., 2009). Hence, concerns about the safety of food production have been raised due to the rapid consumption of phosphate resources (Dawson and Hilton, 2011). Considering that the continued reliance on large P fertilizer inputs to meet the rising demand for food is unsustainable in the future, it is essential to trace the flow of P utilization in crop farming to improve cognition of intensive resources and ensure sustainability of the P resource.

Efforts to identify the P flow are not new. Initially, the rapid migration of P into the terminals of input and output has attracted attention (Landers, 2008). Hence, previous studies have mainly evaluated P flows in farming (e.g., Bast et al., 2009; Chen et al., 2009), production (e.g., Herzog et al., 2008; Senthilkumar et al., 2012) and consumption (Qiao et al., 2011) systems from the perspective of mass balance. A wider interest in P flow is now emerging in response to the abovementioned concerns of resource scarcity and food security. The materials-use efficiency (MUE) concept presented by Hashimoto and Moriguchi (2004) was extended to the phosphorous use efficiency (PUE) concept. PUE represents the efficiency of P recovery from applied P sources, and this parameter is meaningful for the nutrient cycle (Xin et al., 2017). Moreover, the sustainable supply of P for future food security depends not only on the reliable material balance, but also on better utilization efficiency. For crop farming systems, improving the PUE to better manage P resources is one of the key factors that guide crop-farming systems toward more technological, efficient and sustainable agricultural practices. Consequently, several studies have measured the PUE. Childers et al. (2011) and Simpson et al. (2011) evaluated the PUE to determine field vulnerability levels and proposed means of preventing erosion. Nilsson (1995) developed a P budget for the Swedish municipality using the PUE method. Iital et al. (2003) and Kobayashi and Kubota (2004) employed the PUE method to evaluate P losses in water environments. However, these studies were based on material balance and treated the systems as “black boxes”. Hence, it is difficult to identify the sources of impacts on PUE without conducting a life-cycle analysis.

Consequently, the substance flow analysis (SFA) method is proposed as a fundamental tool for evaluating P flows and identifying the PUE (Brunner, 2010). This method systematically assesses the flows and stocks of one substance within a system that is defined in space and time, connecting the sources, pathways, intermediates and final sinks of the substance (Brunner and Rechberger, 2003). Correspondingly, researchers have published meaningful SFA results concerning the PUE in agriculture-related systems on global (Bouwman et al., 2009), national (Cooper and Carliell-Marquet, 2013), watershed/provincial (Wu et al., 2014) and city (Schmid Neset et al., 2008b) levels.

Rice, wheat and maize are the main food staples for more than half of the world's population, especially in China (Wang et al., 2014), where the yield of rice, wheat and maize in 2014 reached 208.2, 130.18 and 22.46 million tons, contributing 28%, 17% and 22% of the world's total yield, respectively (FAOSTAT, 2014). Unfortunately, climate change and its impact on PUE, limiting the capacity of farmers to increase crop production, is a big challenge that China and the rest of the world will have to face. Additionally, the vulnerability of crop production to human interference has become of key concern, with extensive studies conducted on simulating the impact of human interference on crop production worldwide, especially in China (e.g., Smil, 2000; Wu et al., 2015; Wu et al., 2016; Xin et al., 2017). However, past assessments have mostly focused on the impacts of human interference (e.g., Ridoutt et al., 2013; Suh and Yee, 2011; Wu et al., 2014), and few studies have assessed the joint influences of human interference together with climate change. Moreover, most assessments have explored the responses of PUE in the historical period, considering that the reliable estimation of the future impacts of human interference and climate change on PUE is of increasing importance and has become more pronounced, suggesting that it is necessary to employ neural networks and GCMs to evaluate the future responses of PUE to the impacts of human interference and climate change. Consequently, as important parameters to calculate PUE and significantly affect agricultural activities (Smil, 2000; Wu et al. 2015, 2016; Xin et al., 2017), precipitation has been selected as a climatic factor, as well as the crop yield, arable area, sown area and effective irrigation area as the agricultural practice factors to assess the responses of PUE to the climate change and human interference, respectively. Hence, the corresponding results will be helpful to the agricultural management department to adopt adaptive measures in the future. This is greatly meaningful and practical. The findings are expected to help identify major barriers to the efficient use of P in crop farming systems in the middle and lower reaches of the Yangtze River (MLRYR) in China during 2001–2030.

Therefore, the objectives of the present study are to (1) quantify and compare the PUE of past and future periods of three main crops; (2) explore how future human interference and climate change have impacted the PUE with multiple neural networks and GCMs, which enables the assessment of human interference and climate change impacts with fixing management practices to respond to the challenges in P security; and (3) determine the potential causes of variations in PUE for every influence factor related to the human interference and climate changes examined. To this end, a widely used empirical PUE model (Wu et al. 2014, 2015) was employed with corresponding agricultural statistics and meteorological data. In addition, the statistical down scaling method (SDSM) was used to create daily weather series from the GCMs.

2. Methods and data

2.1. Study site description

The Yangtze River is regarded as the “Natural Moat” because it is the longest river in China running from west to east. Located in central and eastern China (between 111°E–123°E and 27°N–34°N), the MLRYR are the main component of the “Yangtze River economic zone” (see Fig. 1). This area consists of seven provinces (i.e., Shanghai, Jiangsu, Zhejiang, Anhui, Jiangxi, Hubei and Hunan, ordered from east to west). The climate of this region is of the subtropical monsoon type with summer rainfall from June to August. The mean annual precipitation is 1000–1400 mm, and the annual mean temperature varies from 14 °C to 18 °C.

Furthermore, this region is an important manufacture base of China, including steel, machinery, electric power, textile and chemical, etc. Moreover, the agricultural industry of the area is well developed, the land reclamation index is at a high level, and it is an important base for grain, cotton and oil. In 2015, the GDP, population and crop yield of the MLRYR were US$ 3456.7 billion, 393 million people and 16 million tons, respectively, accounting for

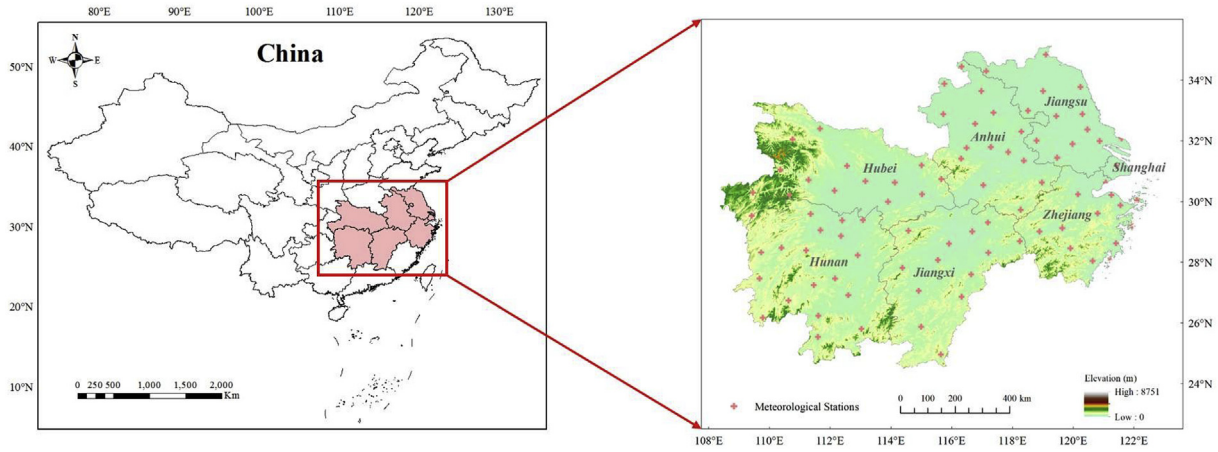

Fig. 1. Maps of the middle and lower reaches of the Yangtze River (MLRYR) and locations of the meteorological experimental stations.

approximately 34%, 29% and 26%, respectively, of the corresponding totals in China.

The MLRYR are selected as the study area because of the following reasons. First, the study regions cover an area of 200,000 km^2, of which 51,926,097 ha is cropland, comprising 32,735,124 ha of rice, 13820123 ha of wheat and 5,370,849 ha of maize. Hence, in this region, agricultural production is highly intensive, and this area also has a population of 393 million and thus represents one of the most densely populated areas in which human activities significantly affect the P use and discharge (Yuan et al., 2014). Second, this area presents significant agricultural features (i.e., growing of the three major crops rice, wheat, and maize) and therefore consumes large quantities of P fertilizer, while phosphate rock reserves used to produce chemical fertilizers in the area are limited (Wu et al., 2014). However, the PUE of crop farming in the MLRYR is low overall. There can be little doubt that increasing the efficiency of P use is an approach to mitigate the adverse impacts associated with P consumption. Consequently, there is a need to assess the PUE of crop farming from the perspectives of both the historical and prospective in this region. The results of the present study may provide valuable experience on mitigating the impacts induced from crop farming and enhancing the PUE for other regions in China and even other countries.

2.2. System boundary

Based on some related studies (Chen and Liao, 2017; Ridoutt et al., 2013; Wu et al., 2012), the crop farming processes in the MLRYR have been defined as system boundaries for the present study. It is assumed that all P flows occurred during the same year and that no time lag existed. The original data and information regarding this study area were collected from 2001 to 2015. The substance flow analysis (SFA) is applied to trace the path of P within the system from 2001 to 2030 and to assess the long-term changes in PUE.

The crops mainly include rice, wheat and maize. The P inputs into the system originate from chemical fertilizers, pesticides, rural residents' excrement applied to the field, livestock excrement applied to the field, air deposition, irrigation and seeds. Additionally, P outputs and stocks from the system include grains, straw and soil deposition, and straw stored in the field (see Table S1 for the classification and description of the flows). The flows associated with the movement of P-containing materials through these sectors were tracked.

As discussed in the Introduction, there are several available references concerning the impacts of human interference on PUE. However, few studies show the direct responses of PUE to the future impacts of human interference and climate change. Therefore, it is meaningful to compare variations of PUE between history and future. In addition, precipitation has been selected as a climatic factor, and the crop yield, arable area, sown area and effective irrigation area have been selected as agricultural practice factors to assess the responses of PUE to the impacts of climate change and human interference, respectively. To calculate the historical PUE, the present study used the PUE-model from mathematically based formulation, which combined the corresponding agricultural statistics and meteorological data. Additionally, three neural networks (BP, GA-BP and PSO-BP) and GCMs have been employed to project the future agricultural practice and climatic factors. Moreover, although the GCM can forecast the future global climate change well, its spatial resolution is low, and this model lacks detailed regional climate information. Thus, it is difficult to generate a reasonable forecast for regional climate. Hence, the PUE model was coupled with GCMs and statistical downscaling (SDSM), which can compensate for the limitations of predicting the regional climate change for GCMs and convert large-scale climate information into regional-scale climate information to realize the predictions of regional climate. The schematic illustration of the computation processes is shown in Fig. 2. The detailed descriptions of quantifying the PUE, multiple neural networks and extraction future precipitation by GCMs are provided below.

2.3. Quantifying the PUE

Based on the law of mass conservation, the flows of P have been governed in the system boundary (Van der Voet, 2002) to ensure that the amount of input P is equal to the amount of output and stock P. The PUE in the crop farming system in the MLRYR from 2001 to 2030 has been analyzed. Detailed parameters and data are provided in the supplementary materials. The PUE is defined in related studies (Wu et al., 2014, 2015; Peterson et al., 2017).

The P use efficiency in crop farming is defined as the ratio of P product output and P stock to the total P input to crop farming (see Equation (1)):

$$PUE = \left(\frac{O_f + S_f}{I_f}\right) \times 100\% \quad (1)$$

where O_f is the P flows of output in crop farming and equals flows of grains and straw feed; S_f is the P flows of stocks in crop farming and

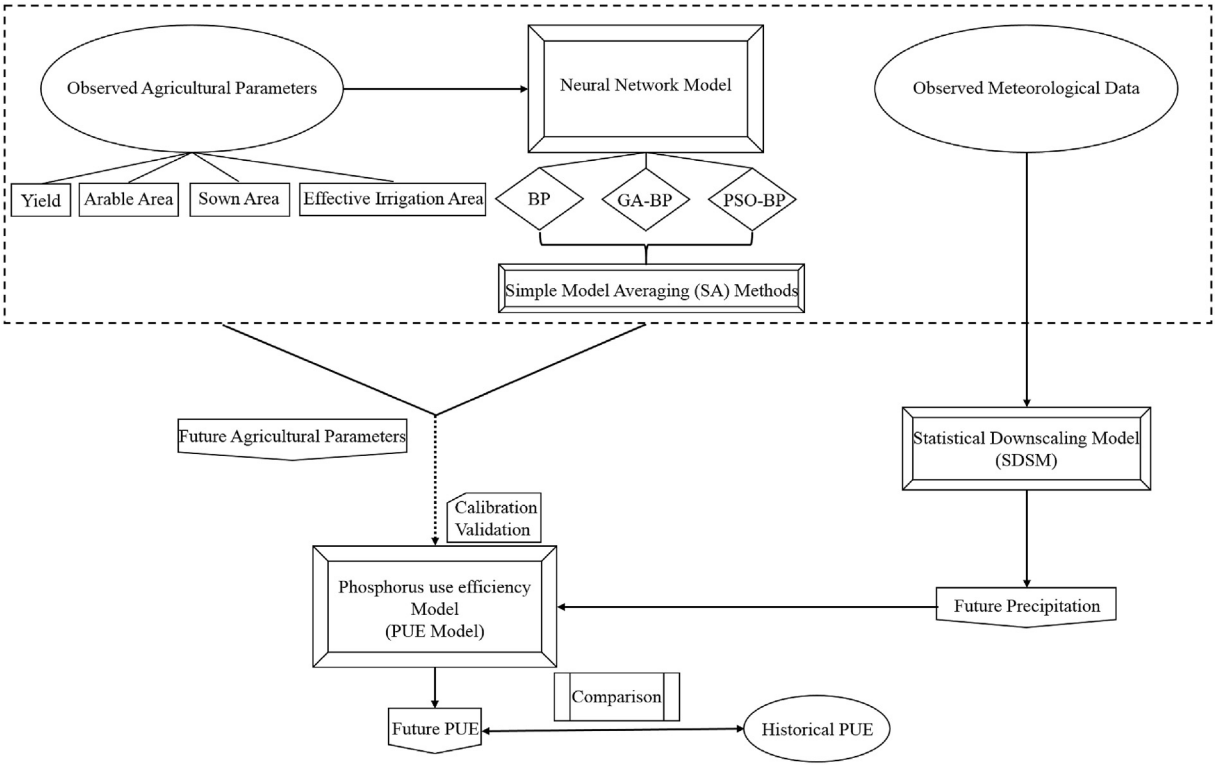

Fig. 2. Schematic illustration of this study.

equals flows of soil deposition and straw stored in the field; and I_f is the total P flows of input in crop farming and equals flows of chemical fertilizers, pesticides, rural residents' excrement applied to the field, livestock excrement applied to the field, air deposition, irrigation and seeds. Details regarding the data and data sources used in the present study are elaborated in Table S2.

2.4. ANN designs for the parameters of human interference

2.4.1. Overview of ANNs

In recent years, soft-computing techniques show great ability in genetic algorithms combined with artificial neural networks for use in analyses and projections of human activity, which are widely used worldwide. For example, a training algorithm according to the evaluation criteria (Kumar et al., 2011) and different artificial neural network approaches, including radial basis function (Kim and Kim, 2008), generalized regression neural networks (Cigizoglu, 2005; Kisi, 2006), back-propagation (Huo et al., 2012), Levenberg Marquardt (Tabari et al., 2013) and conjugate gradient (Landeras et al., 2008), have been adopted in ET_0 modeling. Therefore, forecasting the future variation of crop yield, arable area, sown area and effective irrigation area will be realized by using the genetic algorithm. In the present study, the multi-modal neural networks include BP, GA-BP and PSO-BP. The back propagation (BP) artificial neural network is one of the traditional soft computing learning algorithms, which has strong nonlinear mapping capability and a flexible network structure (Bozorg-Haddad and Marino, 2007; Haro et al., 2012; Liu et al., 2012). However, this method also has disadvantages, for example, slow learning speed and ease of falling into local convergence. In addition, crop yield, sown area, effective irrigation area, and arable area are frequently obtained through ground surveying. Hence, the network structure of the back propagation artificial neural network may be affected by limited data acquisition and uncertain factors (Chen et al., 2013; Raul and Panda, 2013; Wang and Huang, 2014). Correspondingly, to solve the previous problems, the latter two hybrid genetic algorithm neural networks were applied to forecast the variations of human interference and climate change in the future. Additionally, the results of three algorithms based on Simple Model Averaging (SA) methods can be used to determine the uncertain impacts of neural network models and improve the accuracy.

2.4.2. Back propagation neural network (BP)

The BP neural network is a multi-unit feed forward neural network (see Fig. S1). Each neuron is connected to the neurons in the next units, and there is no connection between neurons of the same units. The BP neural network uses the gradient descent method to adjust the weight and threshold value so that the mean square error of the actual output value and the desired output value of the network are minimal. Moreover, the BP neural network has several advantages, such as excellent parallel processing ability, superior nonlinear mapping, and good fault tolerance capability (Zhang and Wu, 2009). Based on these characteristics, the BP algorithm has been widely used in various fields, such as pattern recognition, data prediction, image processing, etc., and its theory development is becoming increasingly mature. Hence, in the present study, the model between time and human interference variables has been established based on the BP neural network.

2.4.3. Genetic algorithm back-propagation neural network (GA-BP)

However, the BP neural network does account for the gradient direction of the previous time in the process of weight correction, making oscillation and slow convergence occur in the learning process. In addition, the BP neural network is highly sensitive to the initial connection weights between the neurons in the input units and the hidden units, the hidden units and the output units, and the initial threshold value of the hidden units and the output units. If these parameters are not reasonable, slow convergence will appear

and the network will fall into a local optimum. Hence, a hybrid BP neural network has been used in the present study. This hybrid network can reduce the oscillation of the learning process, improve the convergence and obtain the global optimal solution by quickly searching the entire solution space by introducing a genetic algorithm.

GA introduces the biological evolution principle "survival of the fittest" to the coding population formed by the optimization parameters. It screens individuals according to the selected adaptation degree function and through selection, crossover and mutation in inheritance, maintains individuals with high adaptation degrees and eliminates individuals with low adaptation degrees. The new population has not only inherited the information of the last generation but is also superior to the last generation, and the cycle will be repeated until the conditions are satisfied. The reciprocal of the absolute value of the difference between the predicted and expected outputs of individuals is regarded as the fitness function, as shown in Equation (2)

$$F = 1 \Big/ \sum_{i=1}^{n_0} |y_i - Q_i| \tag{2}$$

where no denotes the number of neurons in the output layer and y_i and Q_i denote the predicted and expected outputs of the ith neuron, respectively. Then, the number of neurons in the hidden layer can be obtained by performing the operations of genetic algorithms, such as selection, crossover, and mutation. The reciprocal of the sum square of the difference between the predicted and expected outputs of individuals is regarded as the fitness function, as shown in Equation (3).

$$F = 1 \Big/ \sum_{i=1}^{n_0} (y_i - Q_i)^2 \tag{3}$$

The initial weights and thresholds of the GA-BP neural network can be obtained according to the above analysis. The roulette method is used as the selection strategy. Namely, the larger the individual fitness value, the greater is the probability of being selected. The intersect operator is a single-point crossover approach. Two individuals are selected from the group according to a certain probability, and parts of the code from each individual are exchanged. Mutated individuals can be selected according to mutation probability. The mutation position is randomly determined. Then, GA is used to optimize the weights and thresholds until the best individual is found. The modeling steps of the human interference model based on the GA-BP neural network are depicted in Fig. S2.

2.4.4. Particle swarm optimization neural network (PSO)

PSO is an EC technique that simulates social behaviors such as bird flocking or fish schooling. The principle of this technique is based on the social interaction of birds in the group, for which thinking is not only personal but also social to search randomly for food in the area. Each bird is a single solution, and each solution can be illustrated as a particle in the swarm. Each particle moves in the search space to identify the most favorable solutions. Therefore, each particle is specified by its position and velocity in the search space, which are updated based on personal and neighbor experiences. Moreover, the PSO neural network is the most commonly used stochastic population-based evolutionary computation technique inspired by the evolution of nature. The detailed information is expressed as follows:

Step (1): Random generation of initial values of velocity and position.
Step (2): Velocity updating.

The velocities of each particle are updated using the following Equation (4):

$$V_{id}(t+1) = (w^* v_{id}(t)) + (c_1{}^* r_1{}^* (p_{id} - x_{id}(t)) + (c_2{}^* r_2{}^* (p_{gd} - x_{id}(t)) \tag{4}$$

where i represents a particle, t shows the tth iteration in the optimization process, and d indicates the position of the particle in the search space. The w factor is used to evaluate the effect of the previous velocities on the current velocity, which is called 'the inertia weight'. The c_1 and c_2 are the 'acceleration constants'. The r_1 and r_2 factors are the random variables in the range of [0, 1]. The p_{id} parameter is the best previous position of the particle, which is called 'the best personal position', and p_{gd} is the best position acquired by the population, which is called 'the best global position'.

Step (3): Position updating in which the positions of each particle are updated using the following Equation (5):

$$x_{id}(t+1) = x_{id}(t) + v_{id}(t+1) \tag{5}$$

The x (t) vector value is the current position of the particle. In addition, the best global position, p_{gd}, is updated using the obtained fitness by all the particles in the swarm.

Step (4): Termination, where iterations are repeated until the lowest error is obtained (Skvortsov, 2015).

2.4.5. Particle swarm optimization-back propagation neural network (PSO-BP)

With the limitation of convergence of BP, combining the PSO with BP as a hybrid algorithm can improve the accuracy of the projection of parameters. Fig. S3 displays a diagram corresponding to the training method of the neural network using the PSO-BP algorithm. The objective function is the minimum error of the validation and test dataset of simulated agricultural practice factors under implicit conditions (see Equation (6)). The four agricultural practice factors (crop yield, sown area, effective irrigation area, and arable area) were estimated in the PUE model.

$$Z^f_{i,k+1} = M\left(X^a_{i,k}\right) + w_{i,k} \qquad w_{i,k} \sim N(0, Q_k) \tag{6}$$

The superscript f represents the moment of predicting, the superscript α represents the moment of state analysis, subscript k represents the runtime of the model, $Z^f_{i,k+1}$ is the predicted value of the model at the k+1 moment, $X^a_{i,k}$ is the state analysis value of the i th set at time k, M is the model operator of the PUE model, and $w_{i,k}$ is the error of the model.

2.5. Projection of future climatic variables

In the present study, the future climatic variables acquired from three Global Climate Models (GCMs), including HadGEM2-ES, BCC-CSM1.1 (m) and GFDL-ESM2M (see Table 1), were used in the CMIP5 experiment (Taylor et al., 2012). These global climate models were selected since they fully meet the data requirement to force Equation (1) and analyze the future PUE. The GCMs include four different scenarios with RCP2.6, RCP4.5, RCP6.0 and RCP8.5 in

Table 1
Summary of 3 general circulation models used in this study.

Center	Model	Approximate Atmospheric Resolution
Met Office Hadley Center	HadGEM2-ES	1.875° × 1.24°
Beijing Climate Center, China Meteorological Administration	BCC-CSM1.1(m)	1.125° × 1.125°
Geophysical Fluid Dynamics Laboratory	GFDL-ESM2M	2.5° × 2°

which RCP2.6 is a low so-called peak-and-decay scenario (Radiation force reaches a maximum near the middle of the 21st century before falling to 2.6 W m^{-2}), RCP6.0 and RCP4.5 are two intermediate scenarios (Radiation force stability of 6.0 W m^{-2} and 4.5 W m^{-2} by 2100, respectively), and RCP8.5 is a high emissions scenario (Radiation force increases to 8.5 W m^{-2} by 2100) (Wang et al., 2017). Considering that the GCMs span the entire 21st century scenarios range, two representative scenarios, RCP4.5 and RCP8.5, have been selected to drive the precipitation data and analyze the future PUE from now to 2030.

2.6. Data resource

The observation period of the present study is 2001–2015. Provincial sown area, crop yield, effective irrigation area, arable area, fertilizer, pesticide, rural population and livestock in the observed years were collected from the China Statistical Yearbook from 2002 to 2016 (NBSC, 2001–2016). Furthermore, crop phenological data for key growing stages were extracted from the 101 agrometeorological experimental stations. Finally, the meteorological data for assessing the response of precipitation to PUE of 94 meteorological stations in 7 provinces of the MLRYR were downloaded from the Climatic Data Center, China Meteorological Administration (http://data.cma.cn/).

3. Results

3.1. Overall human interference factors

The present study selected the crop yield, arable area, sown area and effective irrigation area as human interference factors to assess the PUE in crop farming systems in the MLRYR (see Table 2).

Holistically, the annual crop yield in each province from 2001 to 2015 showed an increasing trend. However, there are differences between regions and crops; taking rice as an example, the yields of the study area increased, except in Shanghai and Zhejiang. In terms of wheat, only the yields in Jiangxi and Hunan declined. Additionally, the yield of maize in Shanghai declined. The statistics show that the sown area proportions increased from 2001 to 2015 in 7 provinces. Specifically, the sown area of rice in Shanghai and Zhejiang; the sown area of wheat in Zhejiang, Jiangxi and Hunan; as well as the sown area of maize in Shanghai decreased during the study period. In the aspect of the effective irrigation area, the holistic situation in the study region increased, except in Shanghai and Zhejiang. Moreover, the effective irrigation area of wheat in Jiangxi and Hunan as well as the maize in Shanghai decreased. Finally, the proportion of arable area in the MLRYR from 2001 to 2015 increased. From the provincial point of view, the arable area of rice in Shanghai and Zhejiang, the wheat in Jiangxi and Hunan, as well as the maize in Shanghai declined during the study period.

3.2. Historical phosphorus use efficiencies

The provincial interannual linear changing rates of Input-Stock-Output-PUE in the crop farming system from 2001 to 2015 is shown as Fig. 3. In general, the total PUE increased during the study period. However, in terms of rice, notably, the PUE of Zhejiang, Anhui, Jiangxi and Hubei decreased and differed among these years. With respect to wheat, the PUE of Jiangxi and Hunan showed a downward trend, and the holistic PUE of maize increased, except in Jiangsu Province, during the study period.

This was mainly because of the flow of P for Input-Stock-Output

Table 2
Average values and changes of the agricultural activity parameters in the MLRYR for the rice, wheat and maize during 2001–2015.

		Crops	Shanghai	Jiangsu	Zhejiang	Anhui	Jiangxi	Hubei	Hunan
parameters	Yield/10000t	rice	91.47	1777.36	662.27	1324.48	1784.94	1559.49	2440.01
		wheat	15.77	917.81	25.03	1067.66	2.72	303.85	10.61
		maize	2.69	220.40	19.95	338.84	8.26	234.69	149.61
	Arable area/1000ha	rice	1090.28	4984.95	2392.13	3564.74	5435.37	3812.43	6845.48
		wheat	395.21	4501.77	180.15	3752.03	25.82	1762.17	78.62
		maize	40.22	942.47	116.00	1214.69	35.92	936.15	504.99
	Sown area/1000ha	rice	111.48	2175.42	969.02	2165.44	3159.63	2015.71	3894.87
		wheat	40.48	1950.73	72.26	2268.45	15.64	920.48	47.61
		maize	4.12	413.09	46.00	730.10	20.57	486.92	288.41
	Effective irrigation area/1000ha	rice	60.96	1098.61	531.27	866.64	1109.10	622.62	1347.82
		wheat	21.70	985.32	39.84	911.08	5.50	286.55	16.28
		maize	2.25	208.51	25.67	294.95	7.24	152.15	99.43
Changes	Yield/%	rice	−51.46	13.28	−51.46	19.53	26.43	19.82	11.94
		wheat	37.10	40.04	−5.52	47.42	−125.19	49.41	−128.63
		maize	−74.29	−3.06	32.09	43.60	51.56	41.46	39.05
	Arable area/%	rice	−44.24	41.08	−30.63	41.27	36.14	34.74	30.26
		wheat	35.53	47.20	−8.40	46.27	−138.56	51.65	−190.92
		maize	−37.90	36.08	40.29	55.00	50.05	58.13	39.81
	Sown area/%	rice	−57.36	12.28	−62.92	12.75	15.98	9.17	11.53
		wheat	29.67	21.39	−35.19	20.18	−213.93	32.70	−274.35
		maize	−50.44	4.84	25.54	33.15	34.28	41.72	22.55
	Effective irrigation area/%	rice	−62.56	13.80	−12.42	34.38	20.74	32.53	15.23
		wheat	27.32	22.76	6.73	39.97	−196.39	50.01	−253.52
		maize	−55.26	6.49	48.62	49.73	38.00	56.71	26.84

in crop farming. For the PUE of maize in Jiangsu Province, calculated using Equation (1), the P flows of inputs and stocks increased, and conversely, the P flows of outputs showed a decreased trend. However, the P flows of inputs ranged from 237032 t P in 2001–300867 t P in 2015, values much higher than the outputs (from 7063 t to 32486 t) and stocks (from 70992 t to 90139 t). Consequently, the PUE of maize in Jiangsu decreased during 2001–2015. Similar results were obtained for the PUE of rice in Zhejiang as well as wheat in Jiangxi and Hunan. Furthermore, in terms of the PUE of rice in Anhui Province, the P flows of inputs, stocks and outputs increased. Nevertheless, their proportions in Equation (1) are different, and the P flows of inputs ranged from 263274 t P in 2001–350707 t P in 2015. In contrast, the P flows of stocks ranged from 78618 t to 104562 t, and the outputs were between 38942 t and 58971 t. In addition, the PUE of rice in Jiangxi and Hubei is similar to that of rice in Anhui.

3.3. Projections of human interference based on ANN

3.3.1. Input parameters

The yearly values for crop yield, arable area, sown area and effective irrigation area during 1981–2015 were used as the datasets for the ANNs. The datasets for three neural networks were divided into two subsets: the training and testing datasets. The training dataset includes data statistics from 1981 to 2012, and the testing dataset includes data from 2013 to 2015. To enhance the reliability of the data, in the ANN prediction model, the peaks have been normalized. Ensuring that the input samples of each ANN have six data points, use the consecutive data for five years to predict the value for the sixth year. Accordingly, the input sample matrix (5×27) and the output sample vector (1×27) can be established. Detailed parameters for constructing the ANNs are shown in Table 3.

3.3.2. Calibration procedures

Considering the reliability of the ANNs, the measured and predicted per unit of yield of three crops with BP, GA-BP and PSO-BP during the validation period (2011–2015) were used to calibrate the network (see Fig. 4). All regressions of the three neural networks show good reliability, as their coefficients of correlation are all larger than 0.95. Moreover, the regression, training and performance of three neural networks as well as the fitness of the GA-BP and PSO-BP neural networks have been demonstrated (Details results were elaborated in Figs. S4–S15).

3.3.3. Future human interference

The important parameters to calculate the future PUE, namely the crop yield, arable area, sown area and effective irrigation area, have been projected by ANNs and represented as Fig. 5 in the form of Box-and-whisker plots during 2016–2030. Holistically, the prediction results of the three neural networks well reflect the law of changing for parameters. In addition, the trends of predicted data by ANNs for human interference of rice, wheat and maize are shown in Table 4. In terms of crop yield, for most provinces, rice and maize are consistently growing, in contrast with wheat. This finding is mainly due to wheat overproduction. In addition, China imports a certain amount of wheat from abroad every year. Moreover, due to the impact of climate change and the promotion of clean energy, some crops represented by maize have become raw materials for producing clean energy. Correspondingly, the changing trends of the sown area are the same as those of the previous crop yields. Additionally, the reliability of prediction with neural network is good. With respect to effective irrigation area, most of the major grain-producing regions present increased trends. This finding is related to a series of national policies, such as

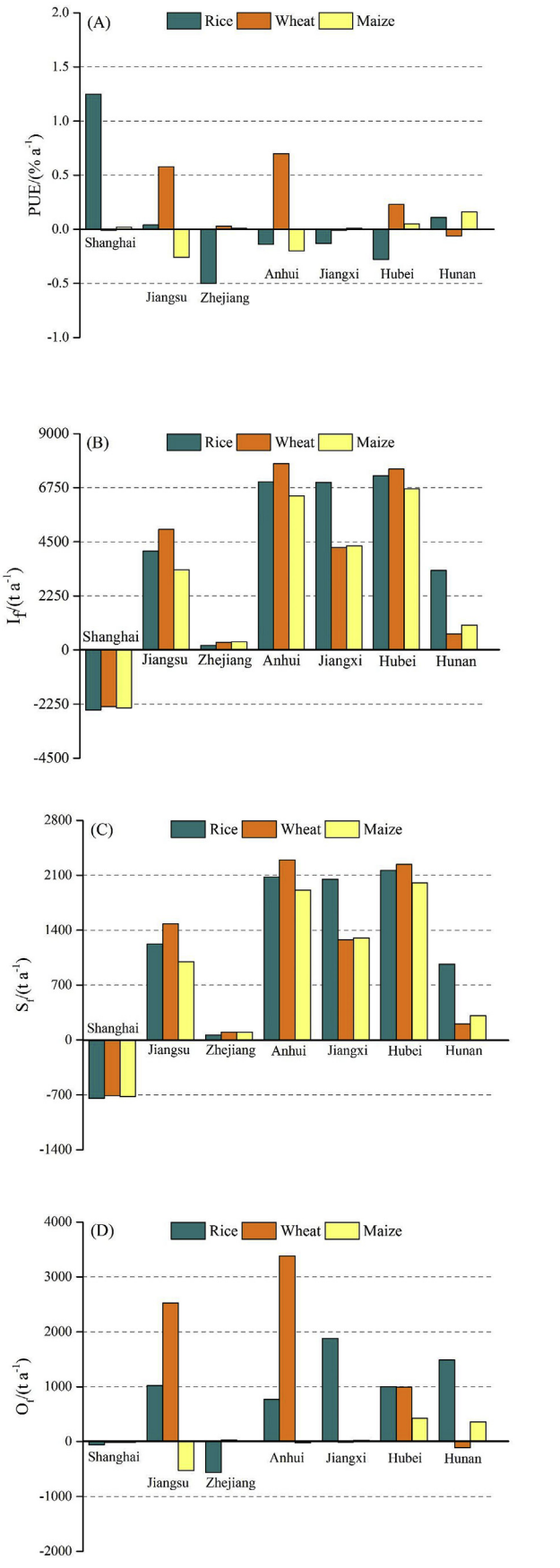

Fig. 3. The provincial interannual linear changing rates of PUE (A), P-flows of Input (B), P-flows of Stock (C) and P-flows of Output (D) in the MLRYR during 2001–2015.

Table 3
Input parameters of ANNs for human interferences of rice, wheat and maize.

Parameter	BP	GA-BP	PSO-BP
Inputnum	5	5	5
Hiddennum	11	11	11
Outputnum	1	1	1
Maxgen	/	120	300
Sizepop	/	50	30
Pcross	/	0.95	/
Pmutation	/	0.001	/
Ggap	/	0.95	/
C_1	/	/	1.49445
C_2	/	/	1.49445
V_{max}	/	/	1
V_{min}	/	/	−1
Popmax	/	/	5
Popmin	/	/	−5
Ws	/	/	0.9
We	/	/	0.4

the development of high standards of farmland, improving the efficiency of agricultural irrigation, etc. Finally, the arable areas of the present study region showed a downward trend due to the rapid development of economy and society, as well as the scarcity of the land resources. Thus, taking their averages, the data predicted by the three neural networks have been used as the input variables of human interference for forecasting the future PUE. The detailed projections with annual values were represented in Fig. S16.

3.4. Projections of PUE with the results of future climate scenarios

In the present study, the impacts of future climate change on PUE, demonstrated as the simulated PUE according to the results of climate scenarios in GCMs, representing a rate of resource utilization, have also been investigated (see Fig. 6). For all seven provinces, despite obvious differences in the changing amplitude between the different RCP scenarios and future stages, the PUE would experience a consistent increase. Concurrently, with the decrease of precipitation, the magnitude of the PUE gradually increased from 2016 to 2030. The PUE values for rice, wheat and maize increased 0.9%, 7.5% and 0.7%, respectively, under all RCPs during 2016–2030. The maximum PUE of rice, wheat and maize were found in Jiangxi in 2025 under BCC-RCP4.5 with a value of 62.99%, in Anhui in 2026 under Had-RCP4.5, 8.5, BCC-RCP4.5 and GFDL-RCP4.5 with a value of 57.53% and in Anhui in 2023 under BCC-RCP8.5 with a value of 35.87%, respectively. In addition, the minimum PUE of rice, wheat and maize were found in Anhui in 2022 under Had-RCP4.5 with a value of 41.80%, in Jiangxi in 2030 under Had-RCP4.5, 8.5, BCC-RCP4.5, 8.5 and GFDL-RCP4.5, 8.5 with a value of 30.06% and in Jiangxi in 2027 under Had- RCP4.5, 8.5, BCC-RCP4.5, 8.5 and GFDL-RCP4.5, 8.5 with a value of 30.20%, respectively.

4. Discussion

4.1. Comparison with other studies

Accurate accounting of PUE is the basis of P resource management in crop farming systems. The PUE of crops in the present study were compared with those reported in the literature (Table 5). There was no relevant accounting of PUE at the national or the provincial scale of the agricultural system in China reported before 1980, whereas the global research on PUE was reported for 1960–2010, but no specific value for PUE is given. The forms of crop species, methods, regions, boundaries and periods calculated in the studies in the literature are also listed in the tables.

Similar to the crop species and methods studied by Wu et al.

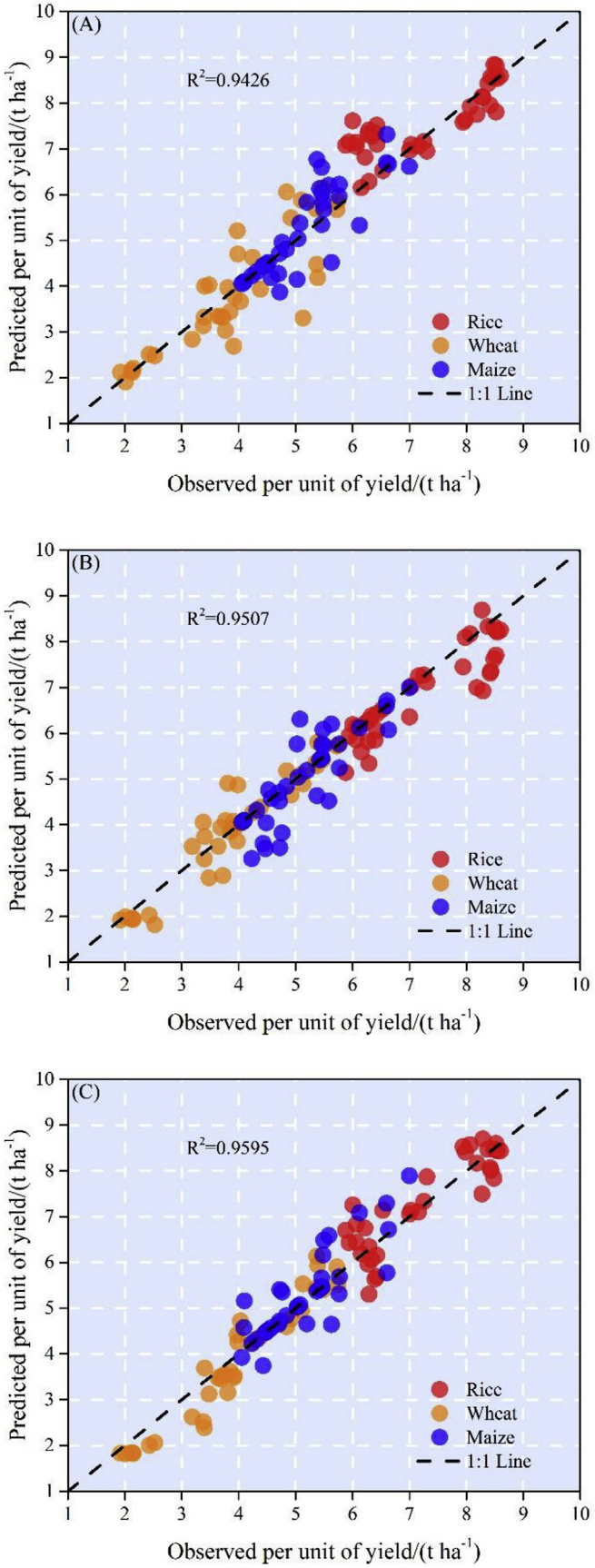

Fig. 4. Measured and predicted per unit of yield with BP (A), GA-BP (B) and PSO-BP (C) during the validation period (2011–2015).

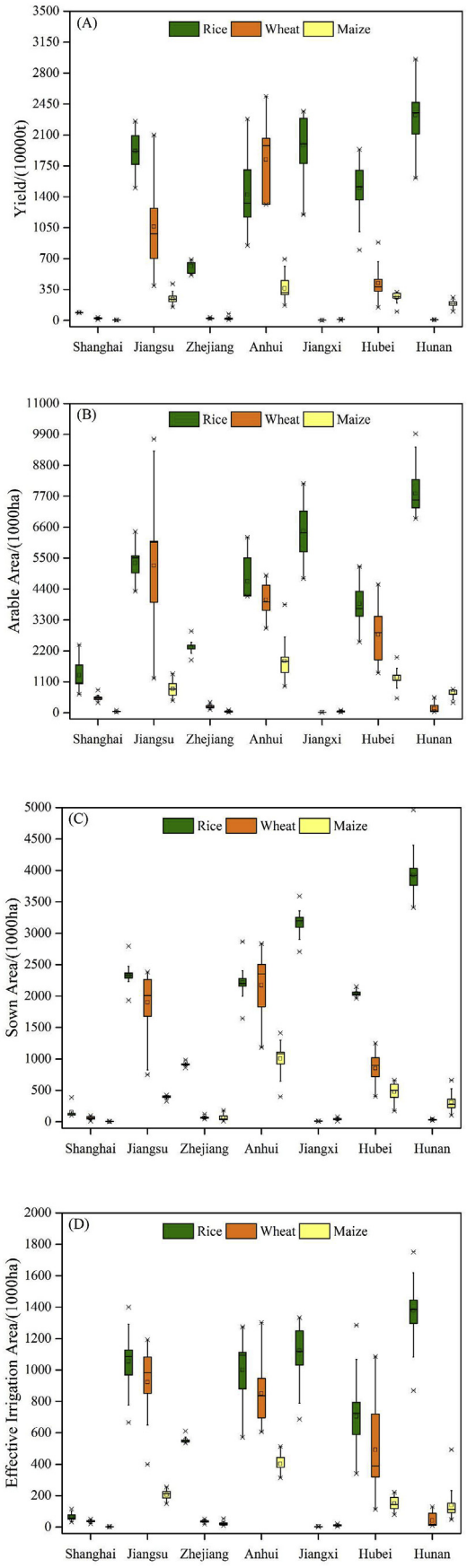

Fig. 5. Box-and-whisker plots for the yield (A), arable area (B), sown area (C) and effective irrigation area (D) projected by three approaches (BP, GA-BP and PSO-BP) for the period of 2016–2030 over the MLRYR.

Table 4
Trends of predicted data by ANNs for human interferences of rice, wheat and maize ("+"represents an increased trend and "-" represents a decreased trend during the predicted period).

Regions	Human interferences	rice	wheat	maize
Shanghai	crop yield	+	−	+
	sown area	+	−	+
	effective irrigation area	+	+	−
	arable area	−	−	−
Jiangsu	crop yield	+	−	+
	sown area	+	−	+
	effective irrigation area	+	−	+
	arable area	+	+	−
Zhejiang	crop yield	+	+	−
	sown area	+	−	+
	effective irrigation area	−	+	−
	arable area	+	−	+
Anhui	crop yield	+	−	+
	sown area	−	+	+
	effective irrigation area	−	+	+
	arable area	−	+	+
Jiangxi	crop yield	+	−	−
	sown area	−	+	−
	effective irrigation area	+	−	−
	arable area	+	+	−
Hubei	crop yield	−	+	−
	sown area	−	+	−
	effective irrigation area	−	+	−
	arable area	−	−	+
Hunan	crop yield	+	+	+
	sown area	+	−	+
	effective irrigation area	+	−	+
	arable area	−	+	−

(2016), three staple grains (rice, wheat and maize) based on substance flow analysis have been analyzed in the present study. However, different from Wu et al. (2016), the present study focuses more on the PUE of agricultural farming. In addition, the present study examines the future response of the PUE to human interference and climate change, which is the most significant difference from other research results. Ridoutt et al. (2013) and Xin et al. (2017) explored the PUE of wheat in Australia's agricultural production system and the wheat-maize system in the north China plain, respectively. Xin et al. (2017) adopted a long-term experiment, while other studies, including Ridoutt et al. (2013), are based on life cycle and substance flow analyses. Nonetheless, both experimental observation and model simulation are based on the principle of material balance. Therefore, the results in the same research boundaries are reasonable. The values for PUE in the crop farming system calculated by Wu et al. (2014) are similar to those determined for the historical period (during 2001–2015) examined in the present study. In addition, from the corresponding research of Wu et al. (2014), compared with the other two systems (rural consumption and livestock breeding), the PUE was lowest for the crop farming system. Ridoutt et al. (2013), Suh and Yee (2011) and Wu et al. (2015) investigated the PUE at a national scale from the perspectives of production and consumption. Wu et al. (2015) analyzed the overall level, while the other two studies focused on agriculture. Moreover, Wu et al. (2015) showed that the holistic PUE of production and consumption in China have increased substantially in the last 30 years. Including this article, Wu et al. (2012), Wu et al. (2014) and Xin et al. (2017) have paid attention to the PUE at provincial and regional scales in China. Moreover, Peterson et al. (2017) and Wu et al. (2016) also examined the agricultural PUE at the watershed scale. This method also provides a way to study the influence of agricultural surface source pollution on the water environment.

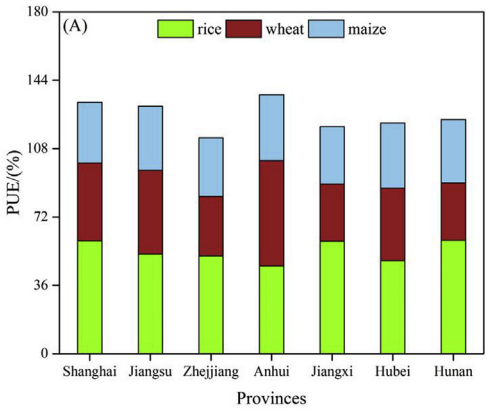

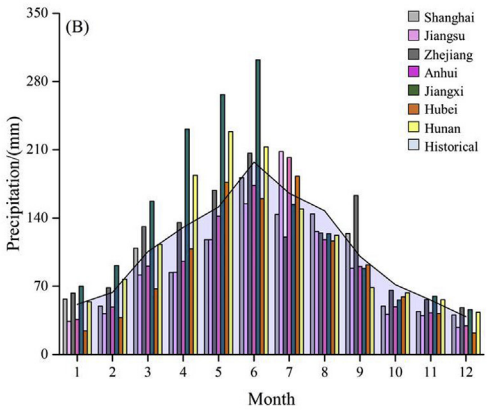

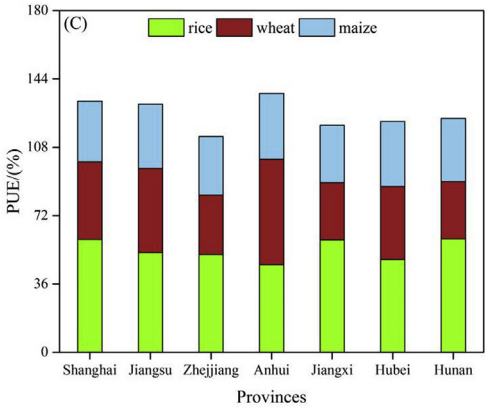

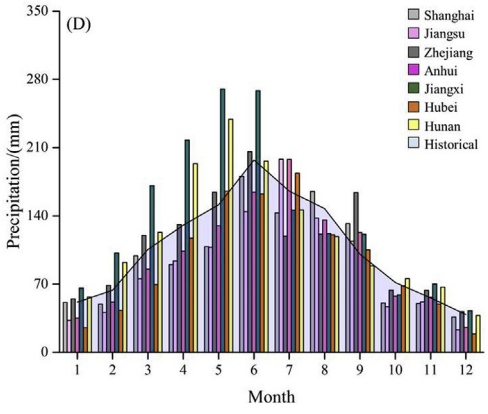

4.2. Uncertain impacts of human interference and climate change on PUE

Increasing at rates of 7.48% and 6.67%, the population and grain output of China grew from 1.248 to 1.341 billion and 512–546 M tons (National Bureau of Statistics of China, NBSC, 2002–2016) over the study period, respectively. This growth makes the P resource scarce, and the quantification of PUE is more significant. PUE represents the utilization efficiency of P and is meaningful for resource saving and food safety. However, the PUE is affected by various factors. In summary, according to the present study, the PUE can be significantly impacted by human interference and climate change, including the crop yield, arable area, sown area, effective irrigation area and precipitation. Moreover, uncertainties exist. In terms of crop yield (A_6 in Table S2), the increase in production will promote the improvement of PUE because the available P is effectively absorbed by the crop and fixed in the roots, and the soil deposition is also enhanced (Ekholm et al., 2005). Furthermore, higher crop yields also produce larger amounts of straw, and the straw stored in the field will be used as straw feed to add to the soil fertility because of the residual P contents (Zhong et al., 2003). Consequently, moderately expanding the crop yield is theoretically beneficial for PUE in this region. From the aspect of effective irrigation area and precipitation (A_{10} and A_{11} in Table S2), the decrease in PUE is mainly due to the erosion of P from irrigation and rainfall to the soil, subsequently causing the loss of P (Chen et al., 2008). However, the parameters that affected the erosion of P, such as the soil erosion rate, rainfall erosive factor and soil erosive factor, are difficult to accurately quantify and are determined from the local natural characteristics. Finally, analyzing the arable area and sown area (A_9 and A_{12} in Table S2), because the seeds contain P, the enlargement of the sown area means an increase in P input (Liu et al., 2008). Moreover, the wind erosion intensity is an important coefficient affecting the PUE, and the increasing arable area will enhance the air deposition, thereby causing a decrease in PUE (Smil, 2000). Furthermore, a high rate of fertilizer is applied to the field, and the application of fertilizer exceeded the absorption by the crops, although some fertilizer was lost to erosion and runoff. This is also one of the reasons for the PUE decline (Ekholm et al., 2005). In addition, Sharpley and Smith (1994) showed that P erosion and runoff might be greatly reduced if nutrients are applied at rates that match crop uptake and if fertilizers are applied while crops are rapidly growing. According to the results of a Chinese investigation, many unseasonable applications of P fertilizer occur on farms, and as a result, less than 40% of farmers apply P fertilizer rationally, and more than 20% of farmers apply P in excess (Wang, 2007). Hence, these previous results suggested that PUE could be improved through changing some planting conditions by human interference.

4.3. Spatial and temporal variation of PUE from historical and future perspectives

In fact, many previous related studies (e.g., Wu et al., 2015; Wu et al., 2016; Xu et al., 2017) have not focused on the impact of climate change on PUE. However, unlike human interference factors, humans cannot fundamentally alter the precipitation to improve PUE (Wang et al., 2013). Hence, predicting the future

Fig. 6. The PUE of three crops under the future two climate scenarios RCP4.5 (A) and RCP8.5 (C). Each histogram reports the mean of HadGEM2-ES, BCC-CSM1.1 (m) and GFDL-ESM2M projections. Monthly average precipitation of MLRYR during 2016–2030 under the scenario RCP4.5 (B) and RCP8.5 (D). Histogram represents monthly mean precipitation of 7 provinces, while gray territory represents historical monthly mean precipitation.

Table 5
Comparison between documented values on PUE of agricultural system with current study.

Document	Crops	Methods	Region	Boundary	Year/period	PUE (%)
This study	Rice, wheat and maize	SFA method and multi-modal neural networks and GCMs	Middle and lower reaches of the Yangtze River, China	Crop farming system	2001–2015 2016–2030	53.61 (rice), 36.22 (wheat) and 32.56 (maize) 54.11 (rice), 38.92 (wheat) and 32.78 (maize)
Suh and Yee, 2011	–	Life-cycle	America	Agriculture and food system	2007	–
Wu et al., 2012	–	Substance flow analysis	Feixi county, China	Socioeconomic system	2008	–
Ridoutt et al., 2013	wheat	Life-cycle	Australia	Agricultural production system	1960–2010	–
Wu et al., 2014	–	Substance flow analysis	Anhui province, China	Farming system	2011	58.79 (crop farming), 71.75 (rural consumption) and 76.65 (livestock breeding)
Wu et al., 2015	–	Life-cycle and substance flow analysis	China	Crop production –consumption system	1980–2012	7.23 (in 1980) and 20.13 (in 2012)
Wu et al., 2016	Rice, wheat and maize	Life-cycle and substance flow analysis	Chaohu Watershed, China	Crop production system	2013	–
Peterson et al., 2017	–	Phosphorus balance	Albert Lea Lake watershed, USA	Agricultural system	2010	1.8 (in total)
Xin et al., 2017	Wheat and maize	Long-term experiment	North China Plain	wheat-maize system	1989–2009	53.7 (in the NPK), 59.9 (in 1/2 OM) and 61.7 (in OM)

rainfall and simulating its impact on PUE can provide a reference basis to effectively improve the PUE from the perspective of human interference. Consequently, the difference between the present study and previous studies is that the former considers both human interference and the impacts of natural variable changes. Comparing the performances of PUE in history (in 2001–2015) and the future (in 2016–2030), the average values of three crops (rice, wheat and maize) in the crop farming system of the MLRYR were calculated and are presented in Fig. 7. These results explicitly illustrated that, from multiple perspectives, the PUE caused by agricultural production increased over time in this region. To maintain the sustainable utilization of P resources, PUE should be improved based on agricultural resource consumption, land use situation and climate change.

4.4. Scope of system boundary and limitation of data

In the present study, the definition of system boundary is different from that proposed in related studies (e.g., Suh and Yee, 2011; Ridoutt et al., 2013; Wu et al., 2016), and the scopes of the

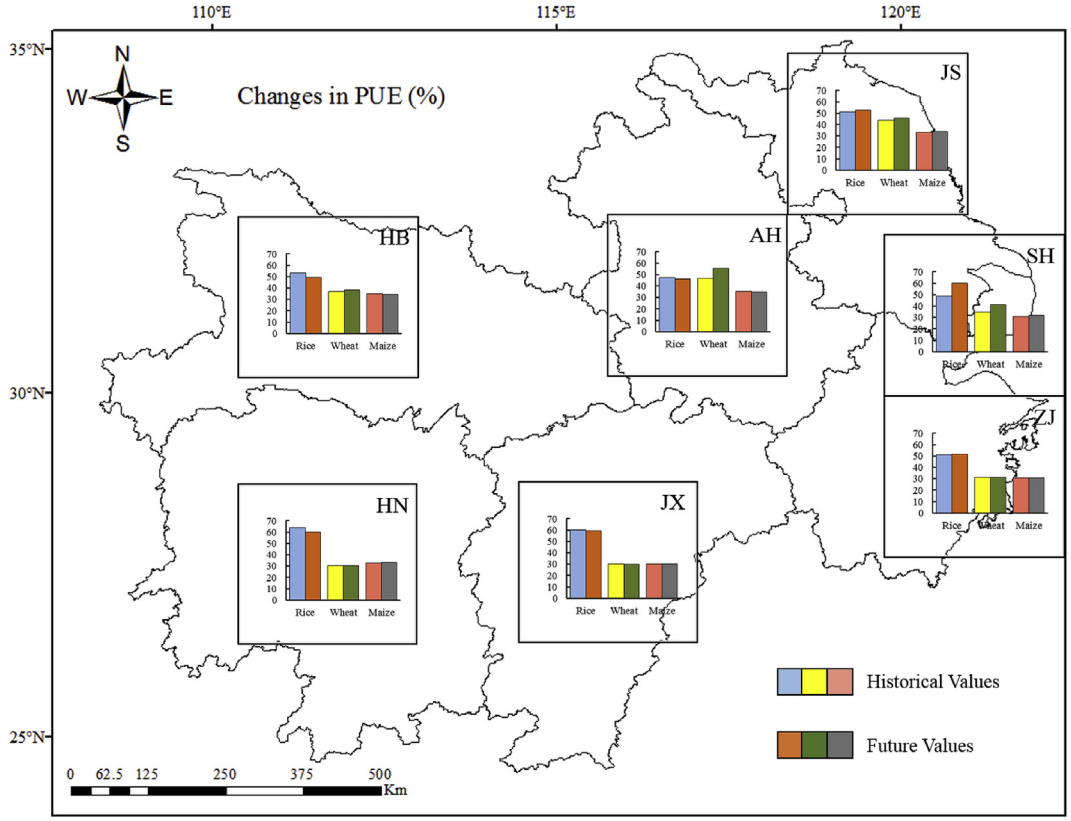

Fig. 7. The variation of interannual PUE in the MLRYR during 2001–2030 (SH: Shanghai, JS: Jiangsu, ZJ:Zhejiang, AH: Anhui, JX: Jiangxi, HB: Hubei and HN: Hunan).

latter studies often involve crop and food systems, including planting, processing and consumption subsystems. However, the scope of the present study focuses on agricultural crop production and not on phosphate rock mining, P fertilizer manufacturing, the influence of the external environment, etc. Additionally, because of the limitation of data, the analytical data collected in the present study were derived from various official government statistics, reports, and scientific studies. Despite efforts to balance and harmonize the information from these often disparate data sources, the relevant information was difficult to obtain; thus, some data regarding imports and exports, i.e., rock mining, manufacturing, seeds and feeds, are subject to varying degrees of limitation.

However, the time scope of the present study was 2001–2030; thus, the P flow was considered as a dynamic process. In addition, the data and results obtained not only reflect the P flows for the historical period but could also be used to accurately reflect the P flows for future years or to measure changes and trends in P flows. Hence, the present results are as meaningful because the spatial and temporal characteristics of the crop farming system in the MLRYR have been selected to conduct a typical and in-depth study.

According to the previous relevant study, the PUE of the crop farming system in China during 1980–2012 were analyzed (Wu et al., 2015). The total PUE was low, at less than 40% during the studied years. Adopting effective methods to explore the future human interference-climate change factors (Wang et al., 2016), including crop yield, arable area, sown area, effective irrigation area and precipitation, then predicting the future response of PUE to human interference and climate change have become the bottleneck when taking appropriate measures to improve PUE.

In the present study, adopting the method combined with the neural network and genetic algorithm to predict future human interference variables. Perhaps, the precision of the constructed model and the accuracy of the prediction are not too high due to the limitations of the data, but this method is a trend to study the changing variables and is worth including in the present study. Furthermore, the future PUE obtained in the present study should not be regarded as the only criterion for selecting technology and techniques, but rather, as only one aspect that might contribute to the improvement of a farming system for use in the MLRYR, China.

5. Conclusion

By analyzing the P flows of the crop farming system in the MLRYR, the present study explored the responses of PUE to the impacts of human interference and climate change from both historical and future perspectives at the province scale. Compared to research results from the previous methods, the most significant differences are that the impacts of climate change on PUE have been considered and the future variations of human interference and climate change have reasonably been projected. Additionally, the sources of these uncertain impacts were analyzed and the spatial and temporal changes in PUE in the study region were shown. Hence, this approach can obtain more accurate and comprehensive results and is helpful for identifying opportunities for agricultural resource management and grain-resource balance, providing additional help for the agricultural management department to adopt corresponding adaptive measures.

Specifically, the results show that compared with wheat and maize, the largest PUE exists in the process of rice planting. Moreover, the average PUE values for the three crops were 53.61%, 36.22% and 32.56%, respectively, in the period of 2001–2015 and 54.11%, 38.92% and 32.78%, respectively, in the period of 2016–2030. However, the overall PUE was low, and there are great differences between interannual variation and regional distribution. Furthermore, the present study highlights the valuable role that human interference and climate change can play in impacting the PUE level. Moreover, this research showed that great potential exists for increasing PUE in this region if corresponding measures can be implemented. Such as, adjusting the land use situation according to crop yield, reducing the amount of irrigation water under the premise of meeting the growth demand of crops, and decreasing the consumption of chemical fertilizers, among other approaches. In addition, optimizing P flows, reducing P losses, and improving PUE throughout the crop farming system by adopting strategic human interference and management measures are all important for the sustainable development of resources and agriculture.

Finally, because the MLRYR present significant agricultural features, the P flows and PUE of its crop farming system might reflect those of other regions. Thus, identifying and analyzing the P flows and PUE from the perspective of history and future might not only provide a basis to conserve resources and, hence, provide a means to develop an ecologically based agriculture for policy-makers but might also demonstrate the analysis of P use in other regions. The results of the present study are important for scientific information on regional agricultural resource management in China.

Acknowledgements

This work was jointly supported by the National Science Foundation of China (51779073, 51609065); the Fundamental Research Funds for the Central Universities of China (2017B21414); the National "Ten Thousand Program" Youth Talent, China; the "Six talent peaks" project in Jiangsu Province, China; the "QingLan Project" of Jiangsu, China and the Priority Academic Program Development of Jiangsu Higher Education Institutions (PAPD), China.

Appendix A. Supplementary data

Supplementary data related to this article can be found at https://doi.org/10.1016/j.jclepro.2018.08.009.

References

Bast, L., Mullen, R., O'Halloran, I., Warncke, D., Bruulsema, T., 2009. Phosphorus balance trends on agricultural soils of the Lake Erie drainage basin. Better Crops Plant Food 6–8.
Bouwman, A.F., Beusen, A.H.W., Billen, G., 2009. Human alteration of the global nitrogen and phosphorus soil balances for the period 1970-2050. Global Biogeochem. Cycles 23, 1–16.
Bozorg-Haddad, O., Marino, M.A., 2007. Dynamic penalty function as a strategy in solving water resources combinatorial optimization problems with honey-bee mating optimization (HBMO) algorithm. J. Hydroinf. 9, 233–250.
Brunner, P.H., 2010. Substance flow analysis as a decision support tool for phosphorus management. J. Ind. Ecol. 14, 870–873.
Brunner, P.H., Rechberger, H., 2003. Practical Handbook of Material Flow Analysis. CRC Press, New York.
Chen, C., Huang, G.H., Li, Y.P., Zhou, Y., 2013. A robust risk analysis method for water resources allocation under uncertainty. Stoch. Environ. Res. Risk Assess. 27, 713–723.
Chen, D.J., Lu, J., Shen, Y.N., Dahlgren, R.A., Jin, S.Q., 2009. Estimation of critical nutrient amounts based on input–output analysis in an agriculture watershed of eastern China. Agric. Ecosyst. Environ. 134, 159–167.
Chen, L., Liao, H., 2017. Engineering crop nutrient efficiency for sustainable agriculture. J. Integr. Plant Biol. 59 (10), 710–735.
Chen, M., Chen, J., Sun, F., 2008. Agricultural phosphorus flow and its environmental impacts in China. Sci. Total Environ. 405, 140–152.
Childers, D.L., Corman, J., Edwards, M., Elser, J.J., 2011. Sustainability challenges of phosphorus and food: solutions from closing the human phosphorus cycle. Bioscience 61 (2), 117–124.
Cigizoglu, H.K., 2005. Application of generalized regression neural networks to intermittent flow forecasting and estimation. J. Hydrol. Eng. 10, 336–341.
Cooper, J., Carliell-Marquet, C., 2013. A substance flow analysis of phosphorus in the UK food production and consumption system. Resour. Conserv. Recycl. 74, 82–100.
Cordell, D., Drangert, J.-O., White, S., 2009. The story of phosphorus: global food security and food for thought. Global Environ. Change 19, 292–305.
Dawson, C.J., Hilton, J., 2011. Fertiliser availability in a resource-limited world:

production and recycling of nitrogen and phosphorus. Food Pol. 36, S14–S22.
Ekholm, P., Turtola, E., Gronroos, J., Seuri, P., Ylivainio, K., 2005. Phosphorus loss from different farming systems estimated from soil surface phosphorus balance. Agric. Ecosyst. Environ. 110, 266–278.
FAOSTAT, 2014. http://faostat.fao.org.
Haro, D., Paredes, J., Solera, A., Andreu, J., 2012. A model for solving the optimal water allocation problem in river basins with network flow programming when introducing non-linearities. Water Resour. Manag. 26, 4059–4071.
Hashimoto, S., Moriguchi, Y., 2004. Proposal of six indicators of material cycles for describing society's metabolism: from the viewpoint of material flow analysis. Resour. Conserv. Recycl. 40, 185–200.
Herzog, F., Prasuhn, V., Spiess, E., Richner, W., 2008. Environmental cross-compliance mitigates nitrogen and phosphorus pollution from Swiss agriculture. Environ. Sci. Pol. 11, 655–668.
Huo, Z., Feng, S., Kang, S., Dai, X., 2012. Artificial neural network models for reference evapotranspiration in an arid area of northwest China. J. Arid Environ. 82, 81–90.
Iital, A., Loigu, E., Vagstad, N., 2003. Nutrient losses and N & P balances in small agricultural watershed in Estonia. Nord. Hydrol. 34 (5), 531–542.
Kim, S., Kim, H.S., 2008. Neural networks and genetic algorithm approach for nonlinear evaporation and evapotranspiration modeling. J. Hydrol. 351, 299–317.
Kisi, O., 2006. Generalized regression neural networks for evapotranspiration modelling. Hydrol. Sci. J. 51, 1092–1105.
Kobayashi, H., Kubota, T., 2004. A study on the spatial distribution of nitrogen and phosphorus balance, and regional nitrogen flow through crop production. Environ. Geochem. Health 26 (2), 187–198.
Kumar, M., Raghuwanshi, N.S., Singh, R., 2011. Artificial neural networks approach in evapotranspiration modeling: a review. Irrigat. Sci. 29, 11–25.
Landeras, G., Ortiz-Barredo, A., López, J.J., 2008. Comparison of artificial neural network models and empirical and semi-empirical equations for daily reference evapotranspiration estimation in the Basque Country (Northern Spain). Agric. Water Manag. 95, 553–565.
Landers, J., 2008. Halting hypoxia. Civ. Eng. 78, 54–65.
Liu, D.D., Guo, S.L., Chen, X.H., Shao, Q.X., Ran, Q.H., Song, X.Y., Wang, Z.L., 2012. A macro-evolutionary multi-objective immune algorithm with application to optimal allocation of water resources in Dongjiang River basins, South China. Stoch. Environ. Res. Risk Assess. 26, 491–507.
Liu, Y., Villalba, G., Ayres, R.U., Schroder, H., 2008. Global phosphorus flows and environmental impacts from a consumption perspective. J. Ind. Ecol. 12, 229–247.
Nilsson, J., 1995. A phosphorus budget for a Swedish municipality. J. Environ. Manag. 45, 243–253.
Peterson, H.M., Baker, L.A., Bruening, D., Nieber, J.L., Ulrich, J.S., Wilson, B.N., 2017. Agricultural phosphorus balance calculator: a tool for watershed planning. J. Soil Water Conserv. 72, 395–404.
Qiao, M., Zheng, Y.M., Zhu, Y.G., 2011. Material flow analysis of phosphorus through food consumption in two megacities in northern China. Chemosphere 84, 773–778.
Raul, S.K., Panda, S.N., 2013. Simulation-optimization modeling for conjunctive use management under hydrological uncertainty. Water Resour. Manag. 27, 1323–1350.
Ridoutt, B.G., Wang, E., Sanguansri, P., Luo, Z., 2013. Life cycle assessment of phosphorus use efficient wheat grown in Australia. Agric. Syst. 120, 2–9.
Schmid Neset, T.S., Bader, H.P., Scheidegger, R., Lohm, U., 2008. The flow of phosphorus in food production and consumption – Linkoping, Sweden, 1870-2000. Sci. Total Environ. 396, 111–120.
Schmid Neset, T.S., Bader, H.P., Scheidegger, R., Lohm, U., 2008b. The flow of phosphorus in food production and consumption – Linkoping, Sweden, 1870-2000. Sci. Total Environ. 396, 111.
Scholz, R.W., Ulrich, A.E., Eilitta, M., Roy, A., 2013. Sustainable use of phosphorus: a finite resource. Sci. Total Environ. 461, 799–803.
Senthilkumar, K., Nesme, T., Mollier, A., Pellerin, S., 2012. Regional-scale phosphorus flows and budgets within France: the importance of agricultural production systems. Nutrient Cycl. Agroecosyst. 92, 145–159.
Sharpley, A.N., Smith, S.J., 1994. Wheat tillage and water-quality in the southern plains. Soil Tillage Res. 30, 33–48.
Simpson, R.J., Oberson, A., Culvernor, R.A., Ryan, M., Veneklaas, E.J., Lambers, H., Lynch, J.P., Ryan, P.R., Delhaize, E., Smith, F.A., Smith, S.E., Harvey, P.R., Richardson, A.E., 2011. Strategies and agronomic interventions to improve the phosphorus-use efficiency of farming systems. Plant Soil 349, 89–120.
Skvortsov, A.N., 2015. Estimation of rotation ambiguity in multivariate curve resolution with charged particle swarm optimization (CPSO-MCR). J. Chemometr. 28, 727–739.
Smil, V., 2000. Phosphorus in the environment: natural flows and human interferences. Annu. Rev. Energy Environ. 25, 53–88.
Smit, A.L., Bindraban, P.S., Schröder, J.J., Conijn, J.G., Meer, H.G.V.D., 2009. Phosphorus in Agriculture: Global Resources, Trends and Developments, 2009 (Report Plant Research International). Plant Research International, Wageningen, p. 282.
Suh, S., Yee, S., 2011. Phosphorus use-efficiency of agriculture and food system in the US. Chemosphere 84, 806–813.
Tabari, H., Grismer, M.E., Trajkovic, S., 2013. Comparative analysis of 31 reference evapotranspiration methods under humid conditions. Irrigat. Sci. 31, 107–117.
Taylor, K.E., Stouffer, R.J., Meehl, G.A., 2012. An overview of CMIP5 and the experiment design. Bull. Am. Meteorol. Soc. 93, 485–498.
Vaccari, D.A., 2011. Sustainability and the phosphorus cycle: inputs, outputs, material flow, and engineering. Environ. Eng. 12, 29–38.
Van der Voet, E., 2002. SFA methodology. In: Ayers, R.U., Ayers, L.W. (Eds.), The Handbook of Industrial Ecology. Edward Elgar, Cheltenham, UK.
Wang, J.Q., 2007. Analysis and evaluation of yield increase of fertilization and nutrient utilization efficiency for major cereal crops in China. In: PhD Thesis. China Agricultural University, Beijing (in Chinese).
Wang, S., Huang, G.H., 2014. An integrated approach for water resources decision making under interactive and compound uncertainties. Omega-Int. J. Manag. Sci. 44, 32–40.
Wang, W., Xing, W., Yang, T., Shao, Q., Peng, S., Yu, Z., Yong, B., 2013. Characterizing the changing behaviours of precipitation concentration in the Yangtze River Basin, China. Hydrol. Process. 27, 3375–3393.
Wang, W., Yu, Z., Zhang, W., Shao, Q., Zhang, Y., Luo, Y., Jiao, X., Xu, J., 2014. Responses of rice yield, irrigation water requirement and water use efficiency to climate change in China: historical simulation and future projections. Agric. Water Manag. 146, 249–261.
Wang, W., Zou, S., Shao, Q., Xing, W., Chen, X., Jiao, X., Luo, Y., Yong, B., Yu, Z., 2016. The analytical derivation of multiple elasticities of runoff to climate change and catchment characteristics alteration. J. Hydrol. 541, 1042–1056.
Wang, W.G., Ding, Y.M., Shao, Q.X., Xu, J.Z., Jiao, X.Y., Luo, Y.F., Yu, Z.B., 2017. Bayesian multi-model projection of irrigation requirement and water use efficiency in three typical rice plantation region of China based on CMIP5. Agric. For. Meteorol. 232, 89–105.
Wu, H., Gao, L., Yuan, Z., Wang, S., 2016. Life cycle assessment of phosphorus use efficiency in crop production system of three crops in Chaohu Watershed, China. J. Clean. Prod. 139, 1298–1307.
Wu, H., Yuan, Z., Gao, L., Zhang, L., Zhang, Y., 2015. Life-cycle phosphorus management of the crop production-consumption system in China, 1980-2012. Sci. Total Environ. 502, 706–721.
Wu, H., Yuan, Z., Zhang, L., Bi, J., 2012. Eutrophication mitigation strategies: perspectives from the quantification of phosphorus flows in socioeconomic system of Feixi, Central China. J. Clean. Prod. 23, 122–137.
Wu, H., Yuan, Z., Zhang, Y., Gao, L., Liu, S., 2014. Life-cycle phosphorus use efficiency of the farming system in Anhui Province, Central China. Resour. Conserv. Recycl. 83, 1–14.
Xin, X., Qin, S., Zhang, J., Zhu, A., Yang, W., Zhang, X., 2017. Yield, phosphorus use efficiency and balance response to substituting long-term chemical fertilizer use with organic manure in a wheat-maize system. Field Crop. Res. 208, 27–33.
Xu, X., He, P., Yang, F., Ma, J., Pampolino, M.F., Johnston, A.M., Zhou, W., 2017. Methodology of fertilizer recommendation based on yield response and agronomic efficiency for rice in China. Field Crop. Res. 206, 33–42.
Yuan, Z.W., Wu, H.J., He, X.F., Liu, X., 2014. A bottom-up model for quantifying anthropogenic phosphorus cycles in watersheds. J. Clean. Prod. 84, 502–508.
Zhang, Y., Wu, L., 2009. Stock market prediction of S&P 500 via combination of improved BCO approach and BP neural network. Expert Syst. Appl. 36, 8849–8854.
Zhong, H.P., Yue, Y.Z., Fan, J.W., 2003. Characteristics of crop straw resources in China and its utilization. Resour. Sci. 25 (4), 62–67 (in Chinese).